01 Mar 2015

Numeric Tuning of Surface Plasmon Enhanced Spontaneous Emission Inducted by Nano-metallic Particle Systems Embedded in GaN-Based LED

Ying Chou Lin
Missouri University of Science and Technology, linyi@mst.edu

Duan Yang Liu

Jin Wei Gao

Recommended Citation

Lin, Y. C., Liu, D. Y., & Gao, J. W. (2015). Numeric Tuning of Surface Plasmon Enhanced Spontaneous Emission Inducted by Nano-metallic Particle Systems Embedded in GaN-Based LED. *IEEE/OSA Journal of Display Technology, 11*(3), pp. 296-303. Institute of Electrical and Electronics Engineers.
The definitive version is available at https://doi.org/10.1109/JDT.2014.2385592

Numeric Tuning of Surface Plasmon Enhanced Spontaneous Emission Inducted by Nano-Metallic Particle Systems Embedded in GaN-Based LED

Yi-Zhu Lin, *Member, IEEE*, Duan-Yang Liu, and Jin-Wei Gao

***Abstract*—In this work, spontaneous emission enhancement inducted by surface plasmon on nano-metallic particle systems embedded in GaN-based LED is investigated numerically. The systems under study consist of two nano-Ag balls or cylinders. By numerically tuning geometrical parameters of the system and polarization of the photon emitting source, we investigate the dependence of spontaneous emission enhancement effect on those factors. It is found that the enhancement magnitude level and peak position are subject to geometrical characteristics of the nano-Ag components in different manners for symmetrical and asymmetrical systems respectively. Higher enhancement ratio for a specific wavelength can be obtained by tweaking parameters of asymmetrical system. Polarization dependence of enhancement effect can be utilized to improve performance of bi-color LED.**

***Index Terms*—Gallium nitride, light emitting diodes, nanophotonics, plasmons, spontaneous emission.**

I. Introduction

NANO metallic particles are not rarely seen in modern optical systems due to their unique optical characteristics. And recent researches have drawn growing attention into their extraordinary properties in relate to surface plasmon (SP) resonance [1]. SPs are quantization of collective oscillations of free-electron gas density on metal/dielectric interface upon the impingement of electromagnetic (EM) waves [2]. SP resonance results in strong confinement of EM field in the vicinity of metal/dielectric interface. This unprecedented ability of confining EM field beyond diffraction limit opens up a wide possibility of manipulating photons and electrons inside opto-electronic devices. For both photon harvesting and emitting devices, SP resonance has seen great potential in improving performances of opto-electronic devices in regard to photon harvesting and emitting abilities. For photon harvesting applications such as sensing and detecting of chemical and biological analytes in the area of food and water safety, medical diagnostics and environment monitoring, etc., significantly enhanced EM field by resonant SP waves can lead to extraordinary sensitivity improvement [3]–[6]. On the other hand, density of states (DOS) of electrons and holes inside photon emitting devices are subject to the modulation of the intensified EM field, which is known as Purcell effect [7]. For photon emitting devices, surface plasmon polaritons (SPPs) create additional decay channel for the excited atoms, resulting in a significant increase of spontaneous emission rate [8]; moreover this additional decay channel is expected to compensate for the loss of efficiency droop [9] of some photon emitting devices such as GaN LEDs at high current injection, which is arguably considered to be caused by Auger recombination [10], [11]. In a nutshell, SP resonance provides solutions to some critical problems of photonic devices and should benefit the efforts of improving photon harvesting and emitting ability.

Being a photon emitting device, LED is hailed as the future source for general purpose lighting [12], [13]. The increase in spontaneous emission rate in GaN LEDs can be achieved by using large overlap quantum well (QW) concept, specifically by using either non-/semi-polar QW [14], large overlap polar QW [15], [16], and ternary substrate [17]. In regard to improving photon emitting ability of LED, SP resonance recently has attracted growing attention in research societies. Both theoretical and experimental work has confirmed the overwhelming effect of enhancing local DOS thus spontaneous emission rate of LED in different frequency regions [18]–[24]. This photon emitting improvement technology is usually achieved by engineering nano-metallic structures either inside or on the surface of LED dies. However, because of the confinement nature of SP wave and its exponential decay in normal direction, neither of those are easy tasks. Extreme care has to be taken in engineering nano-metallic structures in order to achieve spatial overlap of decaying field and photon generation region, which allows only a few tens of nano-meter margin for manipulation, and at the same time other performances of LED such as current distribution and carrier leakage prevention must be maintained. The spontaneous emission enhancement effect depends strongly on the size, distance and shape of the nano-metallic particles and are extremely sensitive [25]–[27]. As a result, the

Manuscript received October 14, 2014; revised December 18, 2014; accepted December 18, 2014. Date of publication December 23, 2014; date of current version February 16, 2015. This work was supported in part by the National Natural Science Foundation of China under Grant 11347218, the National Natural Science Foundation of China under Grant 11304066, the China Postdoctoral Science Foundation under Grant LBH-Z12094, and the China Scholarship Council under Grant 20133050.

Y.-Z. Lin is with EMC Laboratory, Missouri University of Science and Technology, Rolla, MO 65401 USA, on leave from Beijing University of Chemical Technology, Beijing 100029 China (e-mail: linyiz@mst.edu).

D.-Y. Liu is with the Department of Physics and Electronics, Beijing University of Chemical Technology, Beijing 100029 China (e-mail: liudy@mail.buct.edu.cn).

J.-W. Gao is with the Department of Physics, Harbin Institute of Technology, Harbin 150001, China (e-mail: jwgao@hit.edu.cn).

Color versions of one or more of the figures in this paper are available online at http://ieeexplore.ieee.org.

Digital Object Identifier 10.1109/JDT.2014.2385592

structural characteristics of nano-metallic components are of great importance in the sense of achieving considerable spontaneous emission enhancement at an acceptable cost to the other LED system performances. It is worth mentioning that for white lighting applications blue LED based upon GaN materials can work with phosphorus coating to produce white light emission, which is considered to be a promising replacement of many conventional daily lighting sources for energy saving purpose [28]. In this work, we numerically investigate the characteristics of SP waves and related spontaneous emission enhancement performances inducted by nano-metallic particle systems comprised of typical and easy-to-fabricate nano-metallic components such as nano-ball and nano-cylinder embedded in GaN material based LEDs. To the best of the authors' knowledge, relevant work previously published mainly focused on nano-metallic structures with uniform geometry, such as large uniform arrays or films, but work on non-uniform structures was rarely reported. Thus our study features breaking uniformity of the system and including tuning of asymmetrical structures besides symmetrical ones.

The spontaneous recombination of electrons and holes is the result of the overlap of wave functions of carriers in QWs in a quantum physics point of view. However the variation of carrier DOS led by changes of surrounding geometry is analogous to the dependence of antenna radiating power on surrounding medium, and thus can be understood semi-classically [29]–[32]. A. Taflove [33] has clarified their equivalence and provided with rigorous mathematical derivation. As a generalized approach, the electron and hole spontaneous recombination process in LED can be explained in terms of current dipole source emission in the classical Maxwell's equations frame. The DOS is mathematically proportional to the radiated power by a dipole source. This relationship is of great importance since it constructs the fundamental method of quantitatively analyzing spontaneous emission of LED in a classical EM field frame.

II. Numeric Simulation

Based upon the premise that uncoupled SP resonance energy of Ag approaches the photon energy emitted by GaN-based LED, Ag based nano-components are selected in study. The nano-Ag particle system under study is composed of a pair of Ag components of varying shapes embedded in GaN medium. The shapes of components include ball and cylinder which are typical choices in fabrication process. The active region (QW and barrier) of a typical blue GaN LED is a few nanometers thick, and along with the variation of composition of InGaN its emission peak can slightly shift around 450 nm. In order to simulate the photon generation process inside blue GaN LED, the system is excited by a dipole source at a given position inside the region, which is ignited by transient Gausses pulse with a bandwidth around 200 nm and centering at 450 nm so that the bandwidth is wide enough to cover the entire emission spectrum and adequate for an investigation of the transient response of the system in broad wavelength range. Although literature reported that transverse EM emission components are dominant in general GaN blue LEDs grown along c-axis [34], in this numeric investigation the dipole orientation is respectively aligned with the three orthogonal axes of Cartesian coordinate system with the purpose of accounting for any possible radiating components in both in-plane and out-of-plane directions which characterize spontaneous emission process. The system is merged into GaN bulk with dielectric constant $\varepsilon = 6.25$. Due to the incoherent nature of spontaneous emission of LED, the entire region is truncated by absorbing boundary conditions [35] on all the sides. 3D full wave numeric method (a commercial solver by finite integral technique) is employed to calculate evolution of the fields, and frequency responses are obtained by using Fourier transform. For accurate representation of rapidly changing SP field, maximal cell size is limited under 1% of minimal wavelength in medium and sub-cells with finer size are deployed at certain positions as necessary. Monitors are set up for the storage of EM field data during iteration as well as the measurement of total radiating power evaluated on an enclosure face around dipole. It should be noted that the proposed system is dispersive in that the metallic particles have dispersive properties [36]. Hence in the simulation, the dielectric constant of dispersive Ag material is fitted into the promising experimental data [37], which is reliable within the frequency range of interest as shown in Fig. 1.

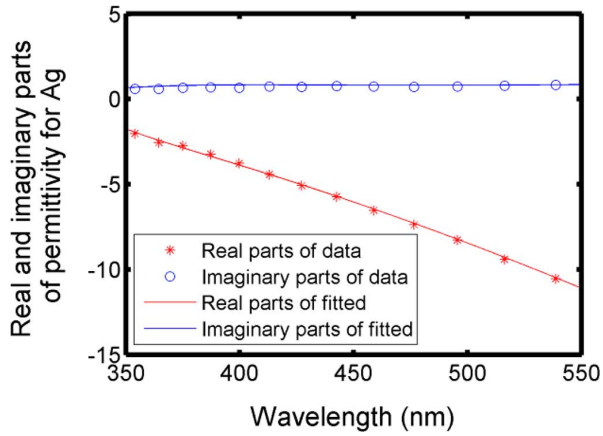

Fig. 1. Comparison of dielectric constants of Ag taken from experimental data and fitted in numeric simulation.

$$DOS_l(x_0,\omega) = -\frac{2}{\pi}\varepsilon(x_0)\frac{Re\left[\widehat{E_l}(x_0,\omega)\widehat{p}(\omega)^*\right]}{\left|\widehat{p}(\omega)\right|^2} \quad (1)$$

The investigation of spontaneous emission enhancement is straightforward since spontaneous emission rate is proportional to DOS, and DOS is equivalent to the power exerted by a dipole source as illustrated in (1). For a given angular frequency ω, DOS at position x_0 in space is exactly proportional to the field $\widehat{E_l}$ generated by dipole $\widehat{p}$ by a factor of $2\varepsilon(x_0)/\pi$ where ε denotes the dielectric constant of the medium [33]. It is worth noting that (1) is normalized with $|\widehat{p}(\omega)|^2$ in order to obtain the radiating power by unit-amplitude dipole source, yet this normalization factor is usually cancelled out since only relative enhancement is concerned most of the time. The spontaneous emission enhancement ratio is thus measured by the variations of the dipole radiating power in nano-particle systems with normalization to a calculation for the same dipole source radiating in homogeneous bulk GaN.

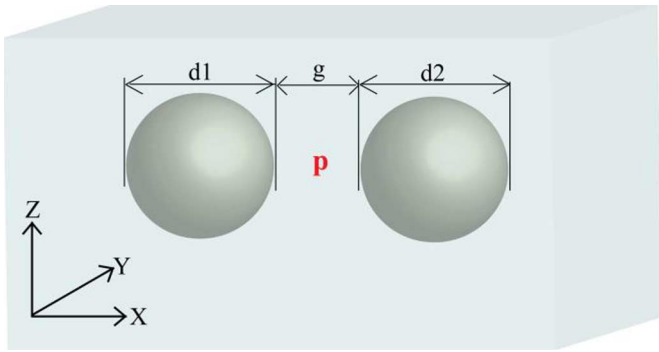

Fig. 2. Schematic of double nano-Ag ball system. Two nano-Ag balls with diameters d_1 and d_2 are separated by a gap g. A dipole p is fired at the center of their spherical center connecting line.

III. Results and Discussions for Nano-Balls

The first nano-Ag particle system under investigation is double nano-ball system. It is worth noting that for Ag/GaN material system, SP fringing field penetration depth into GaN medium is estimated by

$$d = \frac{\lambda}{2\pi}\left[\frac{\varepsilon_{\mathrm{GaN}} - Re(\varepsilon_{\mathrm{Ag}})}{\varepsilon_{\mathrm{GaN}}^2}\right]^{1/2} \tag{2}$$

where ε_{Ag} and ε_{GaN} denote dielectric constants of Ag and GaN, respectively. This penetration depth $d \approx 50$ nm is within the order of a few tens of nano-meters [18]. Therefore recombination centers should be placed at around this range with respect to SP resonant surface where closer range is preferable for greater field concentration. On the other hand, field modulation by SP is only subject to resonance with metallic objects in immediate adjacency with recombination centers whereas out-of-range recombination center and metallic particle pairs are hardly interacted in terms of SP resonance.

The schematic of the system is shown in Fig. 2. Two nano-Ag balls with diameters d_1 and d_2 are separated by a gap g. A dipole p is fired at the center of their spherical center connecting line, which is the position with shortest distance to spherical surfaces. Due to geometrical symmetry, the orientation of dipole is reduced to be either aligned with connecting line (parallel with x-y plane) or perpendicular to it (parallel with y-z or x-z plane).

Fig. 3 plots the enhancement ratio as a function of wavelength for two identical nano-Ag balls separated by a fixed gap $g = 10$ nm. The dipole is placed at the center of their spherical center connecting line with an orientation perpendicular to it. For blue LED, highest enhancement is obtained at $d_1 = d_2 = 50$ nm with a peak positon around 460 nm. For nano-balls with diameter beyond 50 nm, the magnitude of enhancement is decreased as ball diameter increases and blue shift of peak position is also observed (450 nm for $d_1 = d_2 = 70$ nm, 430 nm for $d_1 = d_2 = 90$ nm, and 420 nm for $d_1 = d_2 = 110$ nm), whereas for ball diameter below 50 nm, a red shift of peak position (475 nm for $d_1 = d_2 = 40$ nm) and decline of magnitude are observed with the decrease of diameter. The reversed direction of shift of peak position might be relevant to the start of self-coupling of SP on individual balls. Further decrease of diameter will lead to stronger self-coupling of SP, which renders invalidation of SP energy-momentum dispersion relation. Even with wavelength

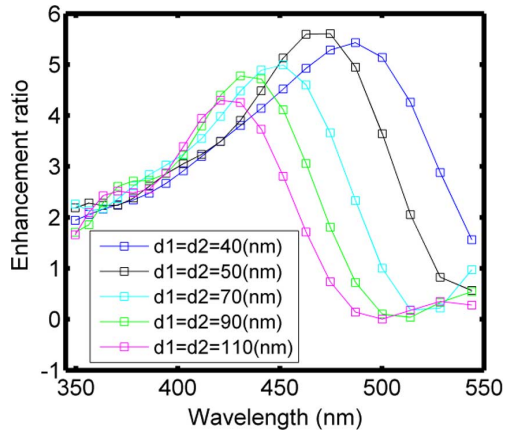

Fig. 3. Enhancement ratio of DOS as a function of wavelength for two identical nano-Ag balls separated by a fixed gap. The dipole is placed at the center of their spherical center connecting line with an orientation perpendicular to it. For ball diameter beyond 50 nm, magnitude of enhancement peak decreases with the increase of ball diameter and blue shift is also observed.

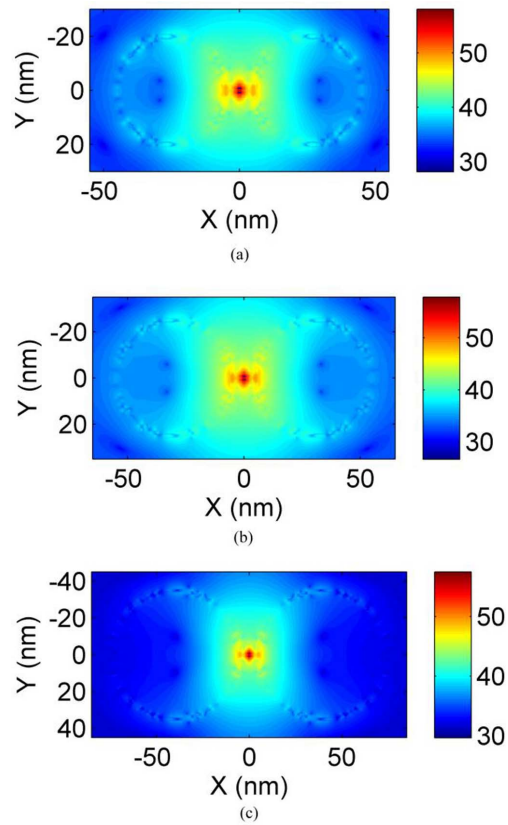

Fig. 4. E-field profiles ($\log_{10}|E|^2$) evaluated on slices cutting through spherical centers in parallel with x-y plane at peak wavelengths for: (a) $d_1 = d_2 = 40$ nm, (b) $d_1 = d_2 = 50$ nm, and (c) $d_1 = d_2 = 70$ nm, respectively, in all of which enhanced SP resonant field can be observed on the surfaces of nano-balls.

shifting and magnitude declining, all the enhancement peaks on the curves feature broadband shape with adequate bandwidth to cover the line-width of typical LED [38].

In order to validate the enhancement led by SP resonance, E-field on the slice cutting through spherical centers in parallel with x-y plane is plotted in Fig. 4. The E-field data are evaluated at the peak wavelengths for (a) $d_1 = d_2 = 40$ nm,

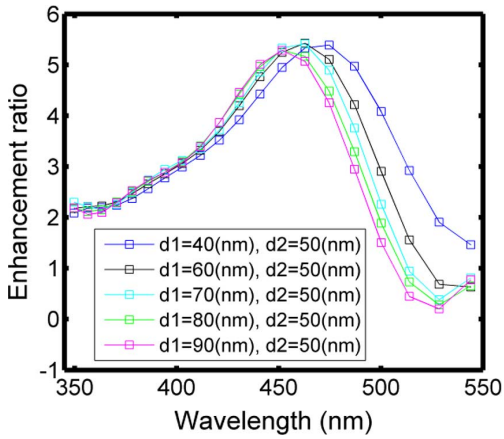

Fig. 5. Enhancement ratio of DOS as a function of wavelength for asymmetrical nano-Ag balls separated by a fixed gap. The dipole is placed at the center of their spherical center connecting line with an orientation perpendicular to it. The diameter of one nano-Ag ball is fixed at 50 nm whereas the other diameter varies from 40 nm to 90 nm. The magnitudes of enhancement peaks approach the same maximal level for varying diameters of nano-balls, yet slight blue shift of peak position is observed with the increase of diameter of one ball.

(b) $d_1 = d_2 = 50$ nm and (c) $d_1 = d_2 = 70$ nm respectively. Enhanced resonant SP field can be seen on the surfaces of nano-balls. The comparison of magnitude can also be distinguished by the profiles where (b) features highest peak intensity and largest area of high intensity region.

Asymmetrical systems are also of interest and investigated by tweaking diameter of one nano-ball whereas keeping the other one constant. Fig. 5 plots the enhancement ratio as a function of wavelength for asymmetrical nano-Ag ball systems separated by a fixed gap $g = 10$ nm. The dipole is placed at the center of their spherical center connecting line with an orientation perpendicular to it. During the tuning procedure, the diameter of one nano-Ag ball is fixed at 50 nm whereas the other diameter varies from 40 nm to 90 nm. For varying diameters of nano-balls, the magnitudes of enhancement peaks approach the same maximal level as the one obtained in the case of two identical nano-Ag balls with diameter of 50 nm, yet slight blue shift of peak positions is still observed with the increase of diameter of one ball. Hence in order to obtain the same high magnitude of enhancement ratio as for $d_1 = d_2 = 50$ nm in two identical nano-ball case in Fig. 1, the diameter of one nano-Ag ball can be fixed at 50 nm whereas the other ball can be tailored by tweaking the diameter for fine tuning of the positon of enhancement peak to match desired wavelength. This dependence of enhancement peak position on asymmetrical geometry, on the other hand, infers that any failure of maintaining uniformity of nano-balls in fabrication process could disrupt enhancement effect, and in high Q factor resonance with narrower and sharper peak shape would possibly result in the mismatch with LED emission peak.

Fig. 6 plots the E-field profiles on slices cutting through spherical centers in parallel with x-y plane at the peak wavelengths for (a) $d_1 = 40$ nm, $d_2 = 50$ nm, (b) $d_1 = 60$ nm, $d_2 = 50$ nm and (c) $d_1 = 80$ nm, $d_2 = 50$ nm of the asymmetrical systems, all of which are obtained by the same procedure as aforementioned. Enhanced SP resonant field can also be seen on the surfaces of nano-balls, and the intensities are at

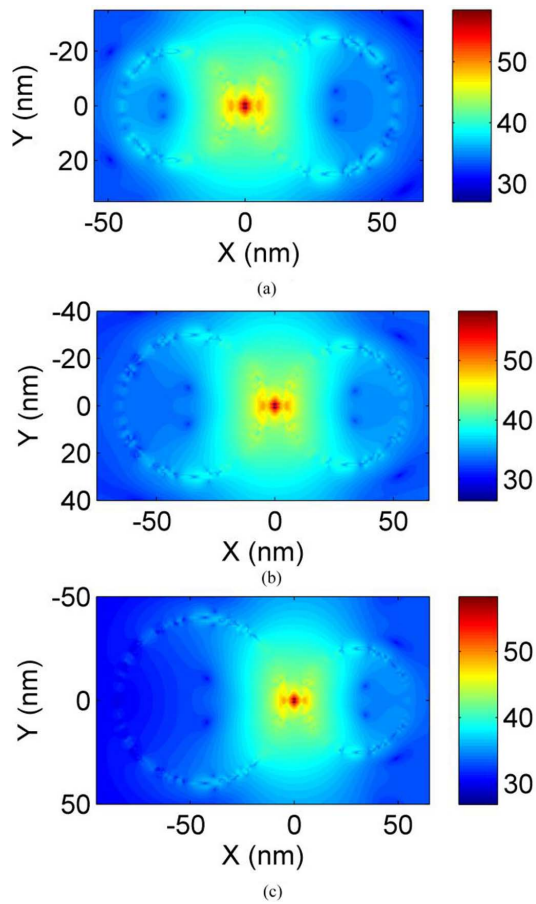

Fig. 6. E-field profiles $(\log_{10}|E|^2)$ evaluated on slices cutting through spherical centers in parallel with x-y plane at peak wavelengths for: (a) $d_1 = 40, d_2 = 50$ nm, (b) $d_1 = 60$ nm, $d_2 = 50$ nm, and (c) $d_1 = 80$ nm, $d_2 = 50$ nm, respectively, in all of which enhanced SP resonant field can be observed on the surfaces of nano-balls, yet with asymmetrical distribution.

the same level. However it is evident that the profiles feature asymmetrical field distribution, in which higher intensity region is constrained on the surface of nano-ball with larger diameter in each pair.

It is worth noting that the enhancement effect is only observed for dipole with orientation perpendicular to the spherical center connecting line. When the orientation is switched to be aligned with the spherical center connecting line, no enhancement phenomenon can be observed. This is due to the polarization selectivity of SP excitation. SP resonance can only be excited by p-polarized light where E-field is parallel with the metal surface. Obviously when the dipole is placed in-line with the spherical center connecting line, E-field component of dipole radiation should be in a direction perpendicular to the ball surface, which invalidates the excitation condition for SP resonance.

IV. Results and Discussions for Nano-Cylinders

In this section, nano-Ag cylinder system is under investigation. The schematic of the system is show in Fig. 7. Two 50 nm high nano-Ag cylinders with diameters d_1 and d_2 are separated by a gap g. The axial directions of both nano-cylinders are aligned with z axis. The height of both cylinders are fixed at 50 nm to avoid self-coupling of SP on individual nano-cylinder.

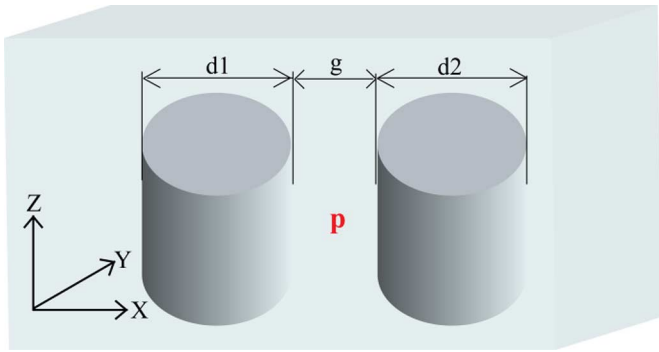

Fig. 7. Schematic of double nano-Ag cylinder system. Two nano-Ag cylinders with diameters d_1 and d_2 are separated by a gap g. A dipole p is fired at the center of their cylindrical body center connecting line.

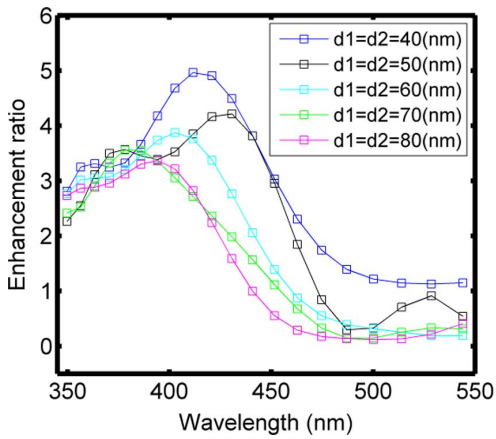

Fig. 8. Enhancement ratio of DOS as a function of wavelength for two identical nano-Ag cylinders separated by a fixed gap. The dipole is placed at the center of their cylindrical body center connecting line with an orientation in-line with y axis. The highest enhancement peak is obtained at around 410 nm for $d_1 = d_2 = 40$ nm. With the increase of cylinder diameter, the peak magnitude declines, and blue shift is also observed.

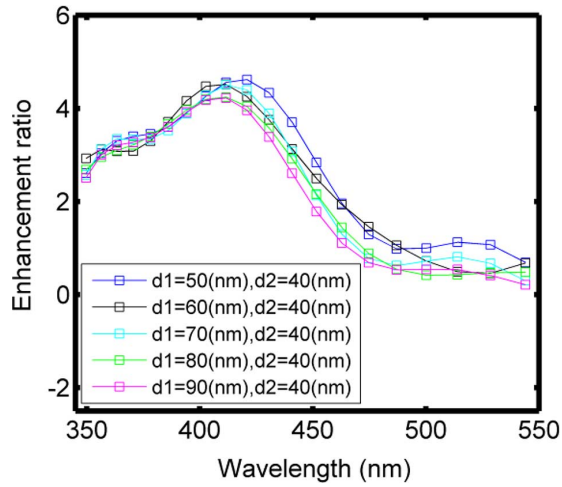

Fig. 9. Enhancement ratio of DOS as a function of wavelength for asymmetrical nano-Ag cylinders separated by a fixed gap. The dipole is placed at the center of their cylindrical body center connecting line with an orientation in-line with y axis. The diameter of one nano-Ag cylinder is fixed at 40 nm whereas the other diameter varies from 50 nm to 90 nm. The magnitudes of enhancement peaks approach a maximal level for varying diameters of nano-cylinders, yet slight blue shift of peak position is observed with the increase of diameter of one nano-cylinder.

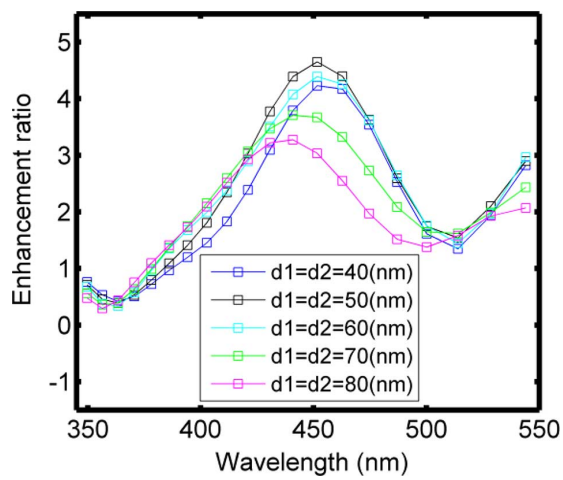

Fig. 10. Enhancement ratio of DOS as a function of wavelength for two identical nano-Ag cylinders separated by a fixed gap. The dipole is placed at the center of their cylindrical body center connecting line with an orientation in-line with z axis. The highest enhancement peak is obtained at 450 nm for $d_1 = d_2 = 50$ nm. For cylinder diameter beyond 50 nm, with the increase of cylinder diameter, the peak magnitude declines, and slight blue shift is also observed.

And a dipole is fired at the center of cylindrical body center connecting line, which is the position with shortest distances to surfaces of both cylinders. The orientation of dipole source is respectively aligned with x, y and z axes.

Fig. 8 plots the enhancement ratio as a function of wavelength for two identical nano-Ag cylinders separated by a fixed gap $g = 10$ nm. The orientation of dipole is aligned with y axis. The highest enhancement peak appears at 410 nm for $d_1 = d_2 = 40$ nm. With the increase of cylinder diameter, the peak magnitude declines. Compared with the two identical nano-Ag balls, the trend behavior of blue shift of peak position remains unchanged, however in a vibrating manner. Moreover the magnitude levels are slightly reduced, and the bandwidths of curves are broadened, which is an indication of slightly lower Q factor of this type of system compared with that of two identical nano-Ag ball system.

Asymmetrical nano-Ag cylinder system is also investigated by fixing the geometrical parameters of one nano-Ag cylinder and tweaking the diameter of the other nano-Ag cylinder only. Fig. 9 plots the enhancement ratio as a function of wavelength for asymmetrical nano-Ag cylinders separated by a fixed gap $g = 10$ nm. The dipole is aligned with y axis. And the diameter of one of the cylinders is fixed at 40 nm for strongest resonance as the one demonstrated in Fig. 8 whereas the other diameter varies from 50 nm to 90 nm. It is evident that the magnitudes of enhancement peaks approach a maximal level as the one obtained in the case of two identical nano-Ag cylinders with diameter of 40 nm. Yet slight blue shift of enhancement peak is still observed with the increase of diameter of one of the nano-cylinders. The general shape of the curves, however, are broader than those in the two identical nano-Ag cylinder system, indicating the change in Q factor.

Fig. 10 plots the enhancement ratio as a function of wavelength for two identical nano-Ag cylinders separated by a fixed gap $g = 10$ nm, yet the orientation of dipole is aligned with

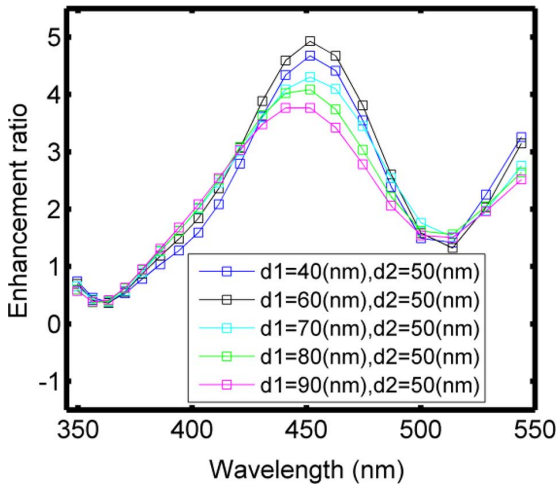

Fig. 11. Enhancement ratio of DOS as a function of wavelength for asymmetrical nano-Ag cylinders separated by a fixed gap. The dipole is placed at the center of their cylindrical body center connecting line with an orientation in-line with z axis. The diameter of one nano-Ag cylinder is fixed at 50 nm whereas the other diameter varies from 40 nm to 90 nm. The positions of peaks are all aligned to 450 nm, yet with decreasing magnitude of peak level as the diameter of one of the nano-cylinders varies from 50 nm to other values. It is evident that no blue shift is observed.

z axis. With nano-cylinder diameter of 50 nm, the highest enhancement peak moves to 450 nm compared with 410 nm obtained by the one with nano-cylinder diameter of 40 nm in Fig. 8. However the magnitude of enhancement peak is slightly lower. For diameter beyond 50 nm, the trend behavior of blue shift of peak position is observed again, however at a slower pace, as evident in the contiguity of the positions of peaks for $d_1 = d_2 = 70$ nm and $d_1 = d_2 = 80$ nm. This phenomenon indicates the peak position is not as much sensitive to the diameter of nano-cylinder as in the case of dipole orientation in-line with y axis.

Fig. 11 plots the enhancement ratio as a function of wavelength for asymmetrical nano-Ag cylinder system with dipole orientation aligned with z axis. The asymmetrical nano-Ag cylinders are separated by a fixed gap $g = 10$ nm, and the diameter of one of the cylinders is fixed at 50 nm for strongest resonance as demonstrated in Fig. 10 whereas the other diameter varies from 40 nm to 90 nm. It is evident that the resonance is dominated by SP on nano-Ag cylinder with diameter of 50 nm as all the curves resemble the curve for $d_1 = d_2 = 50$ nm in Fig. 10. Moreover the positions of peaks are all aligned to 450 nm, yet with decreasing magnitude of peak level as the diameter of one of the nano-cylinders varies from 50 nm to other values. It should be noted that blue shift is not observed in this case due to the insensitivity of peak position to the diameter of nano-cylinder as aforementioned.

To validate the SP nature of the enhancement effect, E-field is also evaluated as shown in Fig. 12. E-field is evaluated on the slice cutting through cylindrical body centers in parallel with x-y plane at peak wavelengths for (a) $d_1 = d_2 = 40$ nm where the orientation of dipole is aligned with y axis, (b) $d_1 = 50$ nm, $d_2 = 40$ nm where the orientation of dipole is aligned with y axis, (c) $d_1 = d_2 = 50$ nm where the orientation of dipole is aligned with z axis and (d) $d_1 = 60$ nm, $d_2 = 50$ nm where the orientation of dipole is aligned with z axis respectively, in all of which highest enhancement ratios are obtained. In each profile, it is evident that enhanced field spots due to SP resonance are observed on the surfaces of nano-cylinders, either with symmetrical or asymmetrical distributions according to the geometries of nano-Ag cylinder system.

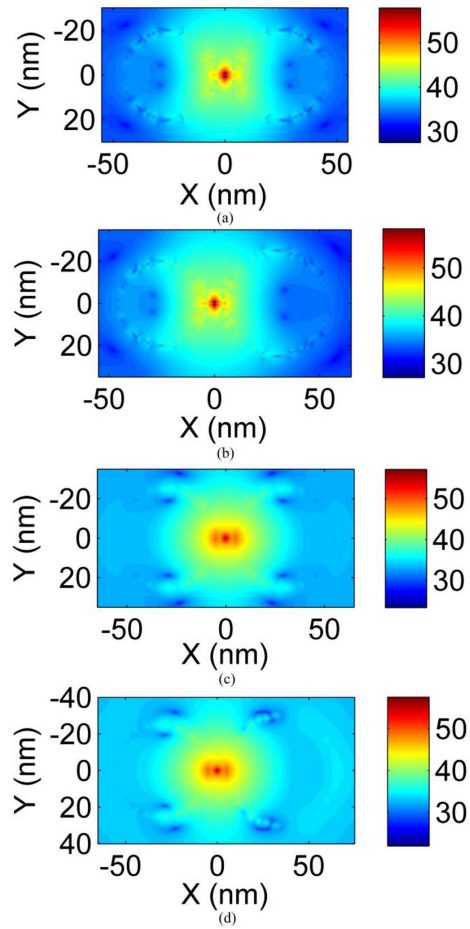

Fig. 12. E-field profiles $(\log_{10}|E|^2)$ evaluated on slices cutting through cylindrical body centers in parallel with x-y plane at peak wavelengths for: (a) $d_1 = d_2 = 40$ nm where the orientation of dipole is aligned with y axis, (b) $d_1 = 50$ nm, $d_2 = 40$ nm where the orientation of dipole is aligned with y axis,(c) $d_1 = d_2 = 50$ nm where the orientation of dipole is aligned with z axis and (d) $d_1 = 60$ nm, $d_2 = 50$ nm where the orientation of dipole is aligned with z axis respectively, in all of which enhanced SP resonant field can be observed on the surfaces of nano-cylinders, either with symmetrical or asymmetrical distributions.

It is also worth noting that for dipole orientation in-line with x axis, no enhancement effect can be observed. This is in agreement with the fact that SP resonance can only be excited by p-polarized incident light where E-field component is in parallel with metal surface. When dipole is placed along x axis, main component of E-field is in the normal of the metal surface, which invalidate the SP excitation condition.

V. Conclusion

In this work, SP resonance enhanced spontaneous emission inducted by nano-Ag particles embedded in GaN-based LED is numerically investigated. The enhancement is achieved by nano-Ag particle systems comprised of typical and easy-to-fabricate nano-metallic components such as nano-balls and

nano-cylinders. Spontaneous emission enhancement system under investigation contains two nano-Ag particles with photon emitter being sandwiched. Symmetrical as well as asymmetrical systems are compared. It can be concluded based upon this study that with either double nano-Ag ball or double nano-Ag cylinder system, significant enhancement of spontaneous emission can be achieved. For systems comprised of two identical nano-Ag balls or cylinders, the enhancement level as well as peak position are subject to the change of geometry of nano particles, and strong enhancement can be achieved at certain wavelengths. Varying the geometrical parameters of nano-Ag particles in symmetrical system can lead to the decline of enhancement magnitude and shifting of peak position. Under certain conditions, in order to obtain a higher enhancement ratio at a given wavelength of interest, asymmetrical systems can be used where the peak magnitude level and position can be tuned by respectively tweaking the geometrical parameters of the two asymmetrical nano-metallic particles. Generally the enhancement effect is polarization sensitive, namely, enhancement can only be obtained for certain orientations of dipole where the E-field component of emitted light wave is in parallel with the surfaces of nano-metallic particles. It also should be noted that for double nano-Ag cylinder system, the enhancement peak position varies for different orientations of dipole, which might be suitable for application in bi-color LED chip.

ACKNOWLEDGMENT

The authors would like to thank Dr. D. Pommerenke, EMC Laboratory, Missouri University of Science and Technology, Rolla, MO, USA, for his generosity and unreserved sharing of his insight into surface waves and knowledge of EM field.

REFERENCES

[1] S. A. Maier, *Plasmonics: Fundamentals and Applications*. New York, NY, USA: Springer, 2010.
[2] W. L. Barnes, A. Dereux, and T. W. Ebbesen, "Surface plasmon subwavelength optics," *Nature*, vol. 424, pp. 824–830, Aug. 2003.
[3] A. Bouali, S. Haxha, F. AbdelMalek, M. Dridi, and H. Bouchriha, "Tuning of plasmonic nanoparticle and surface enhanced wavelength shifting of a nanosystem sensing using 3-D-FDTD method," *IEEE J. Quantum Electron.*, vol. 50, no. 5, pp. 651–657, May 2014.
[4] E. K. Akowuah, T. Gorman, S. Haxha, and J. V. Oliver, "Dual channel planar waveguide surface plasmon resonance biosensor for an aqueous environment," *Opt. Exp.*, vol. 18, pp. 24412–24422, Nov. 2010, 2010.
[5] J. Homola, S. S. Yee, and G. Gauglitz, "Surface plasmon resonance sensors: Review," *Sens. Actuators B, Chem.*, vol. 54, pp. 3–15, Jan. 1999.
[6] E. K. Akowuah, T. Gorman, and S. Haxha, "Design and optimization of a novel surface plasmon resonance biosensor based on otto configuration," *Opt. Exp.*, vol. 17, pp. 23511–23521, Dec. 2009, 2009.
[7] E. M. Purcell, "Spontaneous emission probabilities at radio frequencies," 1946, p. 681.
[8] H. Iwase, D. Englund, and J. Vukovi, "Analysis of the purcell effect in photonic and plasmonic crystals with losses," *Opt. Exp.*, vol. 18, pp. 16546–16560, Aug. 2010, 2010.
[9] M.-H. Kim *et al.*, "Origin of efficiency droop in GaN-based light-emitting diodes," *Appl. Phys. Lett.*, vol. 91, 2007, Art. ID 183507.
[10] J. Iveland, L. Martinelli, J. Peretti, J. S. Speck, and C. Weisbuch, "Direct measurement of auger electrons emitted from a semiconductor light-emitting diode under electrical injection: Identification of the dominant mechanism for efficiency droop," *Phys. Rev. Lett.*, vol. 110, p. 177406, Apr. 2013.
[11] N. I. Bochkareva *et al.*, "Mechanism of the GaN LED efficiency falloff with increasing current," *Semiconductors*, vol. 44, pp. 794–800, Jun. 2010.
[12] S. Pimputkar, J. S. Speck, S. P. DenBaars, and S. Nakamura, "Prospects for LED lighting," *Nat. Photon*, vol. 3, pp. 180–182, 2009.
[13] E. F. Schubert, *Light-Emitting Diodes*, 2nd ed. Cambridge, U.K.: Cambridge Univ., 2006.
[14] D. F. Feezell, J. S. Speck, S. P. DenBaars, and S. Nakamura, "Semipolar $(20\bar{2}1)$ InGaN/GaN light-emitting diodes for high-efficiency solid-state lighting," *J. Display Technol.*, vol. 9, no. 2, pp. 190–198, Feb. 2013.
[15] R. A. Arif, Y.-K. Ee, and N. Tansu, "Polarization engineering via staggered InGaN quantum wells for radiative efficiency enhancement of light emitting diodes," *Appl. Phys. Lett.*, vol. 91, 2007, Art. ID 091110.
[16] H. Zhao, G. Liu, J. Zhang, J. D. Poplawsky, V. Dierolf, and N. Tansu, "Approaches for high internal quantum efficiency green InGaN light-emitting diodes with large overlap quantum wells," *Opt. Exp.*, vol. 19, pp. A991–A1007, Jul. 2011, 2011.
[17] J. Zhang and N. Tansu, "Optical gain and laser characteristics of InGaN quantum wells on ternary InGaN substrates," *IEEE Photon. J.*, vol. 5, 2013, Art. ID 2600111.
[18] L. Yi-Zhu, L. Kang, K. Fan-Min, Z. Jia, D. Liu-Ge, and G. Hui, "Comprehensive numeric study of gallium nitride light-emitting diodes adopting surface-plasmon-mediated light emission technique," *IEEE J. Sel. Topics Quantum Electron.*, vol. 17, no. 3, pp. 942–951, May–Jun. 2011.
[19] C. Hsieh *et al.*, "Localized surface plasmon coupled light-emitting diodes with buried and surface Ag nanoparticles," *IEEE Photon. Technol. Lett.*, vol. 26, no. 21, pp. 1699–1702, Sep. 2014.
[20] C.-Y. Cho *et al.*, "Surface plasmon enhanced light emission from AlGaN-based ultraviolet light-emitting diodes grown on Si (111)," *Appl. Phys. Lett.*, vol. 102, 2013, Art. ID 211110.
[21] N. Gao, K. Huang, J. Li, S. Li, X. Yang, and J. Kang, "Surface-plasmon-enhanced deep-UV light emitting diodes based on AlGaN multi-quantum wells," *Sci. Rep.*, vol. 2, Nov. 2012.
[22] J. Zhu, H. Zhang, Z. Zhu, Q. Li, and G. Jin, "Surface-plasmon-enhanced GaN-LED based on the multilayered rectangular nano-grating," *Opt. Commun.*, vol. 322, pp. 66–72, Jul. 2014.
[23] H. Zhang, J. Zhu, Z. Zhu, Y. Jin, Q. Li, and G. Jin, "Surface-plasmon-enhanced GaN-LED based on a multilayered M-shaped nano-grating," *Opt. Exp.*, vol. 21, pp. 13492–13501, Jun. 2013, 2013.
[24] Y. Kuo, H.-T. Chen, W.-Y. Chang, H.-S. Chen, C. C. Yang, and Y.-W. Kiang, "Enhancements of the emission and light extraction of a radiating dipole coupled with localized surface plasmon induced on a surface metal nanoparticle in a light-emitting device," *Opt. Exp.*, vol. 22, pp. A155–A166, Jan. 2014, 2014.
[25] J. Henson *et al.*, "Enhanced near-green light emission from InGaN quantum wells by use of tunable plasmonic resonances in silver nanoparticle arrays," *Opt. Exp.*, vol. 18, pp. 21322–21329, Sep. 2010, 2010.
[26] J. DiMaria and R. Paiella, "Plasmonic dispersion engineering of coupled metal nanoparticle-film systems," *J. Appl. Phys.*, vol. 111, 2012, Art. ID 103102.
[27] H. Zhao, J. Zhang, G. Liu, and N. Tansu, "Surface plasmon dispersion engineering via double-metallic Au/Ag layers for III-nitride based light-emitting diodes," *Appl. Phys. Lett.*, vol. 98, 2011, Art. ID 151115.
[28] S. P. DenBaars, J. Speck, and S. Nakamura, "Energy savings potential of GaN LEDs for energy efficient lighting and future research directions," in *Proc. Asia Commun. Photon. Conf.*, Beijing, 2013, paper ATh2A.1.
[29] Y. Xu, R. K. Lee, and A. Yariv, "Quantum analysis and the classical analysis of spontaneous emission in a microcavity," *Phys. Rev. A*, vol. 61, Feb. 14, 2000, Art. ID 033807.
[30] R. E. Hamam *et al.*, "Purcell effect in nonlinear photonic structures: A coupled mode theoryanalysis," *Optics Express*, vol. 16, pp. 12523–12537, Aug. 18, 2008, 2008.
[31] Y. Xu, R. K. Lee, and A. Yariv, "Finite-difference time-domain analysis of spontaneous emission in a microdisk cavity," *Phys. Rev. A*, vol. 61, Feb. 14, 2000, Art. ID 033808.
[32] C. Shen, K. Michielsen, and H. De Raedt, "Spontaneous-emission rate in microcavities: Application to two-dimensional photonic crystals," *Phys. Rev. Lett.*, vol. 96, Mar. 2006, Art. ID 120401.
[33] A. Taflove, A. Oskooi, and S. G. Johnson, *Advances in FDTD Computational Electrodynamics: Photonics and Nanotechnology*. Norwood, MA, USA: Artech House, 2013.
[34] D. I. Florescu, D. S. Lee, S. M. Ting, J. C. Ramer, and E. A. Armour, "Edge-emitting electroluminescence polarization investigation of InGaN/GaN light-emitting diodes grown by metal-organic chemical vapor deposition on sapphire (0001)," *J. Electron. Mater.*, vol. 32, pp. 1330–1334, Nov. 2003, 2003.

[35] J.-P. Berenger, "A perfectly matched layer for the absorption of electromagnetic waves," *J. Computational Phys.*, vol. 114, pp. 185–200, Oct. 1994.
[36] V. P. Drachev, U. K. Chettiar, A. V. Kildishev, H.-K. Yuan, W. Cai, and V. M. Shalaev, "The Ag dielectric function in plasmonic metamaterials," *Opt. Exp.*, vol. 16, pp. 1186–1195, Jan. 2008, 2008.
[37] E. D. Palik, *Handbook of Optical Constants of Solids*. New York, NY, USA: Academic, 1991.
[38] T. Chun-Chin *et al.*, "Decay mechanisms of radiation pattern and optical spectrum of high-power LED modules in aging test," *IEEE J. Sel. Topics Quantum Electron.*, vol. 15, no. 3, pp. 1156–1162, May–Jun. 2009.

Yi-Zhu Lin (M'11) was born in Sichuan, China, in 1984. He received the B.S. degree in applied physics from Jilin University, Changchun, China, in 2006, and the Ph.D. degree in radio physics from Shandong University, Jinan, China, in 2011.

From 2011 he was a Lecturer with Beijing University of Chemical Technology, Beijing, China. Since 2014, he is a visiting scholar in EMC Laboratory, Missouri University of Science and Technology, Rolla, MO. His current research interests include design of opto-electronic devices and numeric computation of EM field.

Duan-Yang Liu was born in Hunan, China, in 1985. He received the B.S. degree in applied physics from the College of Science, Tsinghua University, Beijing, China, in 2006, and the Ph.D. degree in condensed matter physics from the Institute of Semiconductors, Chinese Academy of Sciences, Beijing, China, in 2011.

Since 2011, he has been a Lecturer with the Physics Department, College of Science, Beijing University of Chemical Technology, Beijing, China. He is currently engaged in research on semiconductor physics. His research interest includes carrier transport in low-dimensional semiconductor devices.

Jin-Wei Gao was born in Heilongjiang, China, in 1983. He received the B.S. degree in physics from Jilin University, Changchun, China, in 2006, and the Ph.D. degree in optics from Jilin University, Changchun, China, in 2011.

From 2011 to 2014, he was a Post-Doctor with Harbin Institute of Technology, Harbin, China. He is currently a Lecturer with the Department of Physics, Harbin Institute of Technology. His research interests include the applied optics and quantum optics based on interaction of optics and atoms.